



ELSEVIER

Contents lists available at ScienceDirect

## Journal of Solid State Chemistry

journal homepage: [www.elsevier.com/locate/jssc](http://www.elsevier.com/locate/jssc)

# Formation of gold and silver nanostructures within polyvinylpyrrolidone (PVP) gel

Caixia Kan<sup>a,\*</sup>, Changshun Wang<sup>a</sup>, Jiejun Zhu<sup>b</sup>, Hongchen Li<sup>a</sup>

<sup>a</sup> College of Science, Nanjing University of Aeronautics and Astronautics, Nanjing 211100, PR China

<sup>b</sup> National Laboratory of Solid State Microstructures and Department of Physics, Nanjing University, Nanjing 210093, PR China

## ARTICLE INFO

## Article history:

Received 18 November 2009

Received in revised form

20 January 2010

Accepted 22 January 2010

Available online 1 February 2010

## Keywords:

Metal nanostructure

Optical absorption

Crystal growth

PVP

## ABSTRACT

Study on reduction of Au(III) and Ag(I) and the formation of Au and Ag nanostructures was performed on the gels of metal precursor and PVP polymer mixture. Some comparing samples were prepared for better understanding the role of reactants on the reduction of metal ions and further growth of nanocrystals. The results suggest that, in addition to its function of generating stable colloids, PVP not only has a reducing effect on metal ions, but also acts as a crystal growth modifier. At low temperatures, the reducing effect of PVP is strong on Ag(I) ions in AgNO<sub>3</sub>, while the reduction of complex Au(III) ions in HAuCl<sub>4</sub> is slow, involving two steps of Au(III) → Au(I) → Au. In the study of temperature disturbance on crystal growth, Au nanoplates of new and well-defined star shape were observed. The differences in the size and shape of nanoparticles are discussed from the colloid chemistry.

© 2010 Elsevier Inc. All rights reserved.

## 1. Introduction

Noble metal nanostructures have been of an attractive research field because of their size- and shape-dependent colors and optical properties. Known since ancient times, the synthesis of colloidal gold (Au) was originally used as a method of staining glass of wine red, mauve, and blue for particles < 100 nm or yellowish for large particles. These effects are the result of changes in the so-called surface plasmon resonance (SPR) absorption, at which the frequency of free electrons of metals oscillate in response to the alternating electric field of incident electromagnetic radiation [1,2]. The experimental research of Au colloid was pioneered by Turkevich et al. in 1951 [3]. In the past decades, much progress has been made in the synthesis of noble metallic colloids (such as Au and Ag). Experimentally, the metal nanoparticles themselves can come in a variety of morphologies and display characteristic color for different shapes and sizes [4,5]. Thus, the formation and shapes of noble metal nanoparticles can be reflected by the color changes in the colloids.

In recent years, it is found that the SPR absorption of anisotropic Au nanorods, in particular is strong and tunable throughout the visible to near-infrared region in the spectrum. This strong wavelength and polarization sensitivity of the SPR absorption in the near-infrared is an efficient converter of photon energy to thermal energy, which opens new possibilities for many

attractive fields. Currently, a particularly appealing application of the photo-thermal properties is optical recording [6]. Due to their facile synthesis, ease of functionalization, biocompatibility, and inherent non-toxicity, Au nanoparticles are being developed as ideal biological applications, such as gene delivery, cell imaging, photo-thermal therapy and drug delivery technology for delivering anti-cancer drugs [7–14]. And now it is accepted that nanogold does not glitter, but its future looks bright.

For both fundamental aspects and potential technological applications, great efforts have been made to design synthetic methods for producing Au and Ag nanostructures of different morphologies. In recent years, the chemical strategies for the synthesis of noble metal nanostructures have yielded a great deal of literature featuring on the anisotropic growth of crystals into defined morphologies, ranging from rod, plates to highly faceted particles or truncated versions of these shapes [5,15–18]. Among the large number of synthetic methods available, polyol process (ethylene glycol as solvent in most cases) is a convenient, versatile, and low-cost route for the synthesis of metal nanoparticles [19–23]. Metal nanostructures obtained by the polyol method are extremely rich in terms of morphology by changing any parameters in the synthesis system. With the development of colloidal chemistry, this method was improved or modified, through which the pre-formed crystal nuclei can be confined to grow into well-defined anisotropic nanostructures, depending on the experimental conditions and the nature of the pre-formed seeds [23–26].

Although the polyol process is a popular method of preparing metal nanostructures, most of the published works focused on the

\* Corresponding author. Fax: 86 25 52113705.

E-mail address: [cxkan@nuaa.edu.cn](mailto:cxkan@nuaa.edu.cn) (C. Kan).

synthesis itself and on the morphology of nanostructures. In the case of polymer capping agent, such as polyvinylpyrrolidone (PVP), its role is twofold: it acts as a stabilizing agent, preventing aggregation of metal particles and retaining a uniform colloidal dispersion. Additionally, PVP is used as a shape-controlling agent or “a crystal-habit modifier”, promoting attachment of metal atoms onto the specific crystal faces and leading to the highly anisotropic growth of nuclei into nanostructure. As for the reduction mechanism, the published literatures usually discussed the reaction mechanisms involved between the metallic compound and the reducing agent. In the past two decades, there are some different opinions on the topic which reactant is the reducing agent. One is that ethylene glycol (EG) acts as a reducing agent in the polyol method [27]. Recently, it is reported that heating EG molecular results in a kind of reducing agent (glycolaldehyde) in the polyol process [28]. More currently, scientists argued that the capping agents can reduce metal ions to atomic state in the absence of any other reducing agent. It is proposed that the polar groups, such as the  $>C=O$  groups of PVP chain, can interact with metal ions and form coordinating complex, then the compound promotes the formation of crystals once the mixture is dissolved in EG solution [29]. Similarly, in the photochemical reduction of metal ions, PVP was used as a sensitizer in the reduction of copper ions [30].

In this work; We studied the reduction of Au(III) and Ag(I) ions and the formation of their nanostructures by means of optical absorption measurements and color observation on the jellied mixture of metal precursor and PVP polymer (we titled them “gel” hereafter). the gels cannot flow freely; In which solutions of metal precursor filled in the network formed by PVP polymer. More interesting, well-defined Au nanostructures were obtained by a similar method through adjusting the experimental parameters, especially the system temperature of crystal growth. The details are reported in the following.

## 2. Experimental section

Chemical materials of  $AgNO_3$  and  $HAuCl_4 \cdot 3H_2O$ , EG and PVP were purchased from Shanghai Chemical Reagent Co., China and were used directly without further purification. Deionized water used in the experiment was prepared with Millipore purification system (18.2 M $\Omega$ ). Solutions of  $AgNO_3$  and  $HAuCl_4$  with different concentration were obtained by dissolving crystalloid  $AgNO_3$  and  $HAuCl_4$  in deionized water and EG. Here, we assigned the solutions to  $M^{n+}(EG)$  and  $M^{n+}(H_2O)$ , respectively.

### 2.1. Samples preparation

Typically, gels of  $HAuCl_4/PVP$  were prepared at 30 °C by mixing 1 mL  $Au^{3+}(H_2O)$  and  $Au^{3+}(EG)$  ( $[Au^{3+}]=0.05$  M/L) with 1 g PVP, respectively. The molar ratio of PVP repeating unit to  $Au^{3+}$  is about 180. Similarly, gels of  $AgNO_3/PVP$  were also obtained by dropping  $AgNO_3$  solutions ( $Ag^+(H_2O)$  and  $Au^{3+}(EG)$  with  $[Ag^+]=0.2$  M/L) to 1 g PVP, respectively. The molar ratio of PVP/ $Ag^+$  is about 45. Then the gels were immediately prepared for subsequent measurements. Note: if PVP polymer was mixed with EG, the gel is very sticky and loss flowability in a short time, while the mixture of  $H_2O$ -PVP has weak flowability. For optical spectra measurement, the as-prepared gels were sandwiched and sealed by two glass slides to form thin films. For observations on color changes, the wet gels were imported into glass cells with a 5-mm path length. (Here the samples were assigned to 1#:  $Au^{3+}(H_2O)$ -PVP, 2#:  $Au^{3+}(EG)$ -PVP, 3#:  $Ag^+(H_2O)$ -PVP, and 4#:  $Ag^+(EG)$ -PVP, respectively).

For comparisons, the as-prepared  $Au^{3+}(H_2O)$ -PVP gel was kept at both high (80 °C) and low ( $<10$  °C) temperatures to study the temperature influence on the reaction and the final products. To get further information about the effect of EG at high temperature, we added a few drops of  $AgNO_3$  to the heating (150 °C) EG solution without the usage of PVP. Additionally, variability in experimental parameters, such as temperature disturbance, was introduced to the  $Au^{3+}(H_2O)$ -PVP gel during crystal growth. The sample of  $Au^{3+}(H_2O)$ -PVP gel was firstly kept a uniform condition (such as 30 °C for 24 h or 40 °C for 5 h), followed by decreasing temperature (such as from 30 to 20 °C or from 40 to 20 °C). About three days later, Au nanoplates of new and well-defined star shape were observed with high yield.

### 2.2. Characterization

Optical absorption spectra the samples were measured at different time on an SP752-PC ultraviolet–visible (UV–vis) spectrophotometer over the wavelength range from 200 to 1000 nm. Raman spectroscopy technique was performed on NTEGRA Spectra in the range 400–4000  $cm^{-1}$  using laser of 473 nm. The chemical reaction taking place is indicated by the shifting of infrared spectrum bands. X-ray diffraction (XRD) was carried out on an X-ray diffractometer (Ultima-III, Rigaku). The micro images and selected area electron diffraction (SAED) of the samples were characterized by field-emission scanning electron microscope (FE-SEM: ESEM, Sirion200) and transmission electron microscopy (TEM: JEM-1010). For the microstructure measurements, the gels were dissolved in deionized water and centrifugated repeatedly at 3000 rpm to remove (or reduce) the influence of PVP and EG.

## 3. Results and discussions

### 3.1. Color changes and UV–vis spectra analysis

After the gels were prepared, a series of color changes were recorded by digital camera at different times. Fig. 1 shows the color changes of the gels during the polyol process. It can be seen that the color of  $Au^{3+}(H_2O)$ -PVP (1#) and  $Au^{3+}(EG)$ -PVP (2#) change much more slowly than that of  $Ag^+(H_2O)$ -PVP (3#) and  $Ag^+(EG)$ -PVP (4#). The characteristic yellow color of  $HAuCl_4$  in gels of 1# and 2# fades gradually colorless after 4 days (see Fig. 1(a)–(c)). Then the transparent colorlessness turns very slowly to red (the red color of 2# gel enhances slowly with time), as displayed by Fig. 1(d). The 3# gel of  $Ag^+(H_2O)$ -PVP turns from colorless to transparent light brown and further to bottle-green with time. The 4# gel of  $Ag^+(EG)$ -PVP becomes quickly from colorless to opaque salmon pink and further to blue-black for final sample (this color can be seen when the gel was dissolved in water).

Corresponding to the color changes, the time evolutions of optical absorption spectra for the gels were collected, as shown in Fig. 2. Fig. 2(a) is the optical absorption spectra for the thin film of 1# gel sandwiched by two glass slides. In the initial stage, there is an absorption peak around 320 nm, directly originating from d–d transition of the  $AuCl_4^-$  ions [31]. This peak decreases with time and disappears after 60 h, indicating the reduction of  $AuCl_4^-$  ions. However, with the reduction of  $Au^{3+}$  ions, no plasma absorption peak of Au nanostructures can be observed in the spectra. This suggests that  $Au^{3+}$  ions were reduced to a colorless valance state of  $Au^+$  ions or Au atomic state in this stage. The color changes and the optical absorption spectra evolution of 2# gel of  $Au^{3+}(EG)$ -PVP are similar to those of 1# gel, as well as the reported

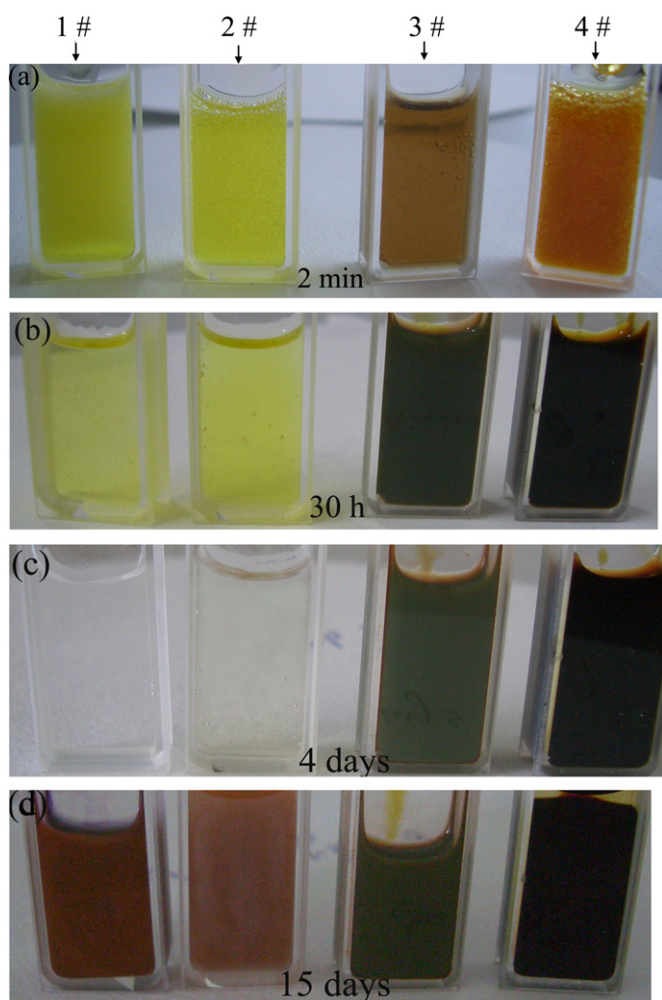


**Fig. 1.** Color changes of the gels with increasing time at room temperature in glass cells with a 5 mm path length. 1#  $\text{Au}^{3+}(\text{H}_2\text{O})\text{-PVP}$ , 2#  $\text{Au}^{3+}(\text{EG})\text{-PVP}$ , 3#  $\text{Ag}^+(\text{H}_2\text{O})\text{-PVP}$ , and 4#  $\text{Ag}^+(\text{EG})\text{-PVP}$ .

evolution of  $\text{HAuCl}_4$  mixed with weak reducing agents [32–36]. About 6 days later, another absorption peak around 580 nm appears and enhances, which originates from SPR of Au nanoparticles, as indicated by curve-1 inserted in Fig. 2(a) for the Au particles colloid centrifugated from 1# gel after 15 days. Curve-2 is the absorption spectrum of Au particles colloid from 2# gel after 15 days, showing an absorption peak at  $\sim 600$  nm, accompanied by absorption with high intensity extending to long wavelength compared with that of 1# gel. According to the color changes and optical absorption spectra, we suggest this process involves a cooperative assembly between the  $\text{HAuCl}_4$  molecule and the PVP polymer synchronized with clear stepwise reduction stages of  $\text{Au}^{3+} \rightarrow \text{Au}^+ \rightarrow \text{Au}$ , and formation of Au nanostructures within the gel.

The optical absorption spectra for gels of 3# and 4# are presented by Fig. 2(b) and (c), respectively. After 2 min, the SPR of Ag nanoparticles at about 420 nm appears for 4# gel of  $\text{Ag}^+(\text{EG})\text{-PVP}$ , while no obvious SPR of Ag nanoparticles can be seen for 3# gel of  $\text{Ag}^+(\text{H}_2\text{O})\text{-PVP}$ . Then with increasing time, the SPR peak ( $\sim 427$  nm for 3# gel) of Ag nanoparticles increases rapidly with time for both samples, indicating fast rates of  $\text{Ag}^+$  ions reduction and Ag nanoparticles formation within the gels. For the spectra of the final Ag nanoparticles colloids from 3# and 4# gels, difference can be seen from their spectra. Inserted in Fig. 2(b) is the absorption spectrum for Ag colloid centrifugated from 3# gel after 15 days. In addition to the SPR of Ag nanoparticles at  $\sim 420$  nm,

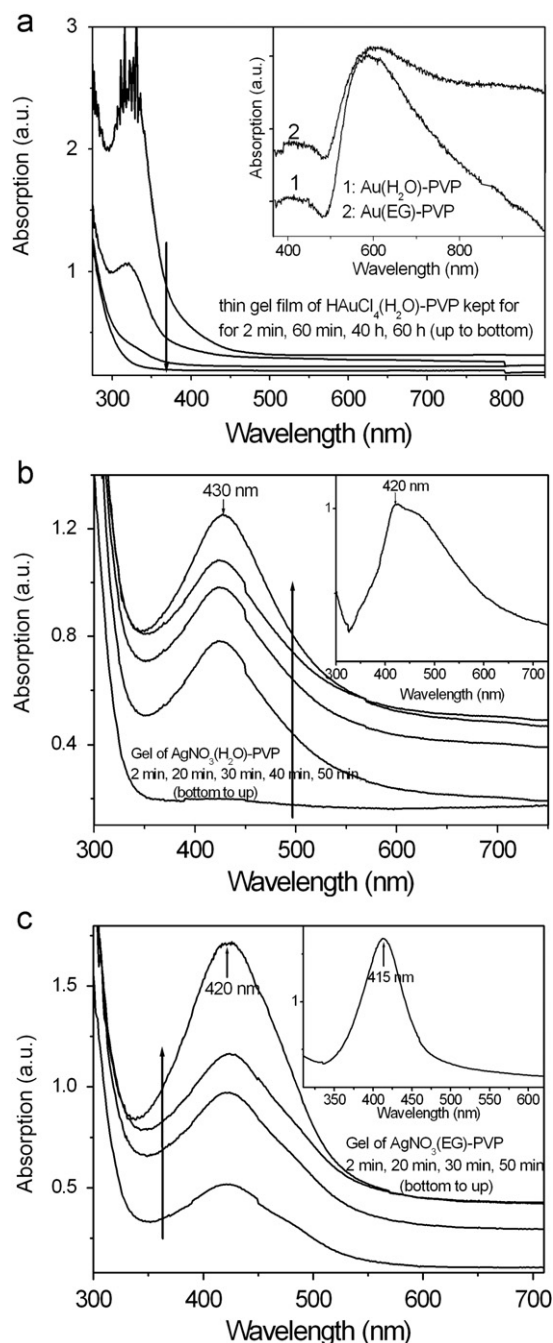


**Fig. 2.** UV-vis spectra for the gels sandwiched by glass slides. (a): 1#  $\text{Au}^{3+}(\text{H}_2\text{O})\text{-PVP}$ , (b): 3#  $\text{Ag}^+(\text{H}_2\text{O})\text{-PVP}$ , and (c): 4#  $\text{Ag}^+(\text{EG})\text{-PVP}$ . Curve-1 and curve-2 inserted in (a): Au particles colloid centrifugated from gels of  $\text{Au}^{3+}(\text{H}_2\text{O})\text{-PVP}$  and  $\text{Au}^{3+}(\text{EG})\text{-PVP}$  after 15 days. Insertions of (b) and (c): Ag particles colloid centrifugated from gels 3# and 4#.

there is an obvious absorption shoulder at  $\sim 470$  nm, indicating the multi-shapes of the final Ag product in 3# gel. However, for Ag nanoparticles colloid from 4# gel, the SPR profile of Ag nanoparticles has no obvious change (The SPR position shifting from 420 to 415 nm should be originated from the environment change of Ag nanoparticles before and after centrifugation).

### 3.2. Microstructure analysis

Fig. 3(a) and (b) are the TEM images of Au nanostructures formed in 1# and 2# gels after centrifugation. In addition to many

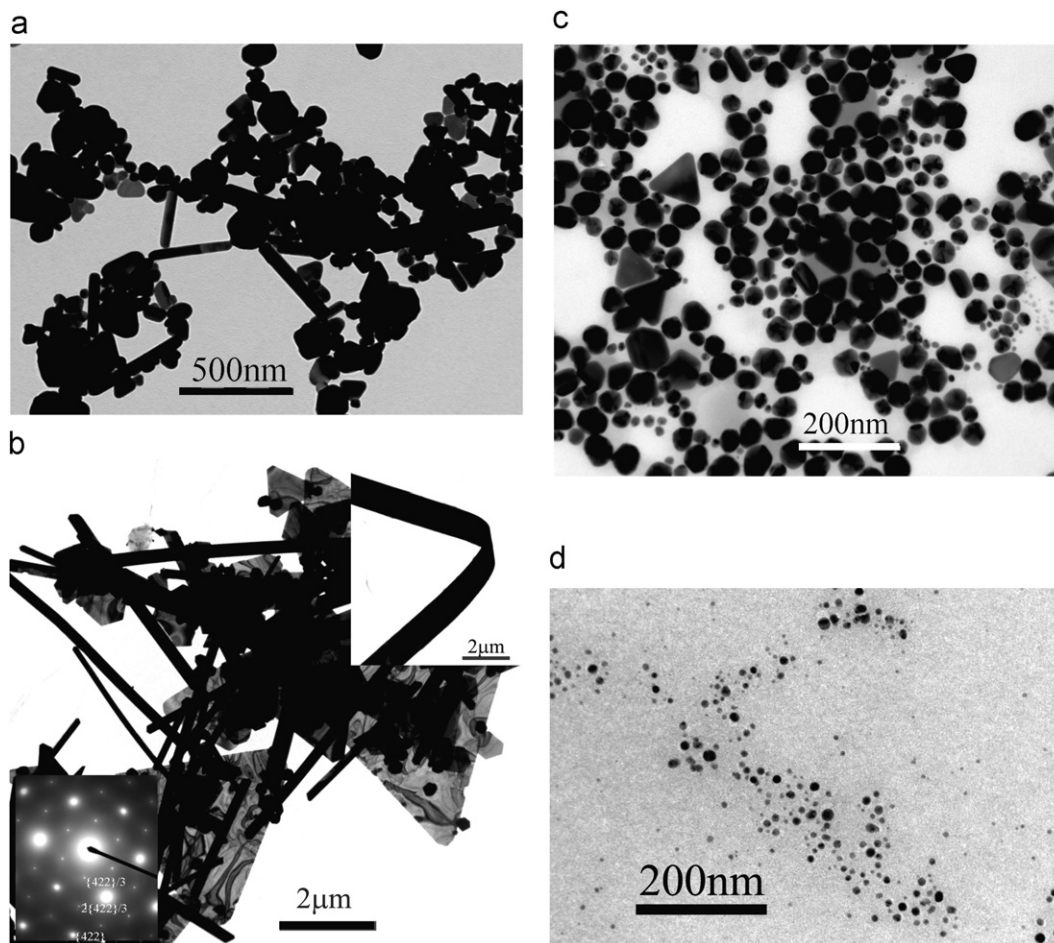


**Fig. 3.** TEM images of Au (a–b) and Ag (c–d) nanoparticles obtained from the gels kept at room temperature. Insertions of (b): down-left one is the SAED of Au nanoplates, and up-right one is one typical Au nanobelts.

Au particles with sizes more than 100 nm, some Au nanoplates, nanorods and nanobelts (figured out from SEM) are observed from 1# gel. However, for Au nanostructures from 2# gel, Au nanoplates, nanorods and nanobelts with larger sizes are the main product. One typical SAED pattern of the Au nanoplates is illustrated by the down-left insertion of Fig. 3(b). The inner set of spots with the hexagonal symmetry was indexed to fractional  $(1/3)\{422\}$  spots, which are commonly observed in  $\langle 111 \rangle$  oriented flat-lying metal nanoplates. The SAED results indicate that the obtained Au nanoplates are single-crystalline, as discussed elsewhere [22]. One typical bended Au nanobelts is presented as an insertion in Fig. 3(b). This morphology difference of Au nanostructures from 1# and 2# gels can be reflected by their optical absorption spectra at wavelength more than 600 nm, as inserted in Fig. 2(a). Studies on the optical properties of Au nanostructures have shown that plasma resonance of Au nanoplates and Au nanorods are located in the near infrared region shifting with aspect ratios [21,37]. Accorded with the absorption spectrum of Ag colloid from 3# gel (insertion of Fig. 2(b)), many kinds of shapes, including rod, plate and sphere, can be seen for Ag nanoparticles from the final product of 3# gel, as illustrated by Fig. 3(c). Whereas, most of the Ag nanoparticles from 4# gel are spherical in shape (see Fig. 3(d)), resulting in the stable SPR profile of the Ag nanoparticles from 4# gel, as illustrated by Fig. 2(c). It is evident that most of the Ag nanoparticles from 3# gel are  $>50$  nm in size, while Ag nanoparticles grow in 4# gel are  $<20$  nm.

In studying the reduction of metal ions in the gels, we found that the reduction of metal ions, especially for  $\text{Au}^{3+}$  ions, is temperature dependent. If the gels were kept at  $80^\circ\text{C}$ , the yellow color of  $\text{Au}^{3+}(\text{H}_2\text{O})\text{-PVP}$  gel turns into colorless after 1 h, and then reddish after 2.5 h (not shown here). However, if the gels were held at a temperature lower than  $10^\circ\text{C}$ , the reduction of  $\text{Au}^{3+}$  ions cannot be detected from the color changes and optical absorption spectra even after 20 days. The color changes on the  $\text{Ag}^+(\text{EG}$  or  $\text{H}_2\text{O})\text{-PVP}$  gels and the corresponding increase on the SPR intensity of Ag nanoparticles become relatively slowly at a low temperature. These results indicate that the reduction of  $\text{Au}^{3+}$  and  $\text{Ag}^+$  ions and the nanoparticles growth in the gels are temperature dependent.

For Au nanostructures grown with temperature disturbance, the products are unexpected, as shown Fig. 4. From the FE-SEM image (see Fig. 4(a)) of sample with temperature changed from  $30$  to  $20^\circ\text{C}$  during crystal growth, we can see that most of the Au nanoplates are star-like with size of several micrometers (The section analysis on AFM image indicated the obtained plates are quite smooth over the width and the thickness of the plates various  $20\text{--}30$  nm). Fig. 4(b) is a TEM images one star-like Au nanoplate, showing a clear morphology of one Au nanoplate with angles of  $3 \times 90^\circ$  and  $3 \times 150^\circ$ . The SAED patterns of different parts of this nanoplate are the same (see Fig. 4(c)), revealing the single crystalline of the nanoplate. In addition to the star-like Au nanoplates, other interesting shapes were found in the sample, as shown in Fig. 4(d) for the plate that contains many steps on the

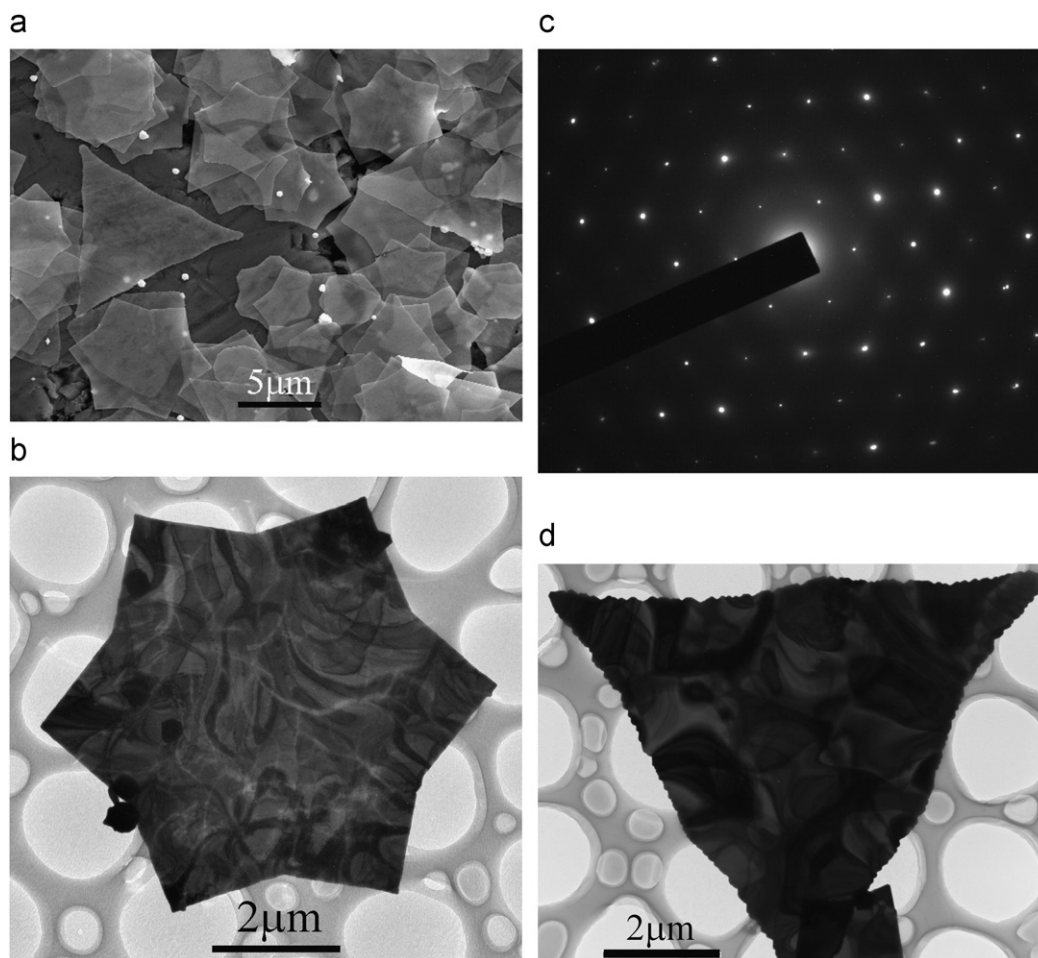


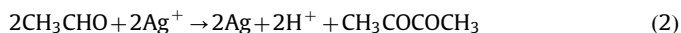
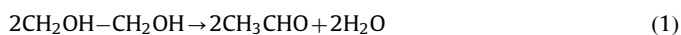
**Fig. 4.** (a) FE-SEM images of Au nanoplates grown with temperature disturbance from 30 to 20 °C. (b–c) TEM image and SAED of one star-like Au nanoplates. (d) TEM image of one Au nanoplate, showing many steps on the lateral surfaces of this morphology.

lateral surfaces (also see the plate of trigonal-star shape but not regular triangular in Fig. 4(a)). Further experiments and analysis about this finding are proceeding.

### 3.3. Which reagent(s) is (or are) the reducing agent(s)?

Based on our experiment results and the reported works, we will present our understanding on the reduction process of  $\text{Au}^{3+}$  and  $\text{Ag}^+$  ions in the gels. Firstly, we turn our attention closely to the question is which reagent(s) is (or are) the reducing agent(s), PVP or EG?

In the past two decades, different opinions about the reduction of metal ions,  $\text{Ag}^+$  ions for instance, were proposed in the polyol process (usually with temperature higher than 100 °C). The first one is that the EG or agent derived from EG is the reducing agent. At high temperature, the molecule of EG ( $\text{CH}_2\text{OH}-\text{CH}_2\text{OH}$ ) may be decomposed to a kind of reducing agent glycollic aldehyde ( $\text{HOCH}_2\text{CHO}$ ) with two aldehyde groups ( $-\text{CHO}$ ) that have strong reductive property [28]. Thus, the opinion that EG plays the role of reducing agent in hot system was proposed with priority, according to the chemical reaction:



This is true for the reduction of  $\text{Ag}^+$  ions in hot EG solution, which was proved in our research work and the reduction proceeds quickly. Fig. 5 compared the Raman spectra of EG

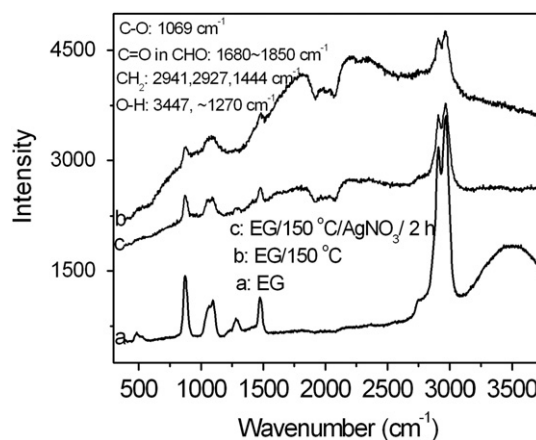


**Fig. 5.** Raman spectra of EG before (a) and after (b) heating at 150 °C. (c) After addition of  $\text{AgNO}_3$  solution to the heated EG solution.

before and after heating at 150 °C (curve-a and curve-b), illustrating the nature of changes in the hydroxyl ( $-\text{OH}$ ) stretching band. After heat treatment, the Raman spectra showed distinct changes. There is a broad absorption throughout the wavenumber. The broad stretching bands of  $-\text{OH}$  centered at  $\sim 3500\text{ cm}^{-1}$  and  $\sim 1270\text{ cm}^{-1}$  decrease obviously. Meanwhile, new stretching band appears at  $1680\text{--}1850\text{ cm}^{-1}$ , indicating the existence of the carbonyl bond ( $\text{C}=\text{O}$ ) in the aldehyde group, as expected by

chemical reaction (1). However, the absorption peak of  $\text{-CH}$  in the aldehyde group at  $\sim 2720\text{ cm}^{-1}$  cannot be detected possibly because it was embedded by the broad absorption background. After addition of  $\text{AgNO}_3$ , the optical absorption spectra showed the quick formation of Ag nanoparticles (not shown here). Except for the damp of the absorption background, the profile of  $\text{C=O}$  absorption at  $1680\text{--}1850\text{ cm}^{-1}$  (curve-c) has no obvious changes, which is accorded with function (2). These results clearly showed that as EG reduces the metal ions, it undergoes oxidation to aldehyde compound firstly and further carbonyl compound. However, in our experiment, no obvious evidence was obtained for the reduction of  $\text{Au}^{3+}$  ions for more than 5 h in hot EG solution.

Recently, with the application of PVP in the polyol process, some groups proposed that PVP has a reducing ability on the metal ions [27,28]. In our experiment, no special reducing agent or treatment was applied, and the EG molecules in the gels are stable at low temperature. Moreover, the gels of  $\text{Au}^{3+}(\text{H}_2\text{O})\text{-PVP}$ ,  $\text{Ag}^+(\text{H}_2\text{O})\text{-PVP}$  and the comparing sample have no EG molecules. Thus, the opinion that EG is the reducing agent is not reasonable for our case when the gels are kept at room temperature. Here, we believed that PVP polymer that usually used as a stabilizer plays an important role on the reduction of metal ions, especially at room temperature.

In the experiment, if some drops of  $\text{Au}^{3+}(\text{EG or H}_2\text{O})$  and  $\text{Ag}^+(\text{EG or H}_2\text{O})$  solutions were dispersed on a glass slides without the usage of PVP, the color changes and the SPR of Au (or Ag) nanoparticles cannot be detected after keeping for a long time, even at a temperature of  $80^\circ\text{C}$ . In order to get further experimental proof for the reduction effect of PVP polymer, the XRD patterns for  $\text{Au}^{3+}(\text{H}_2\text{O})$  without and with the use of PVP dried at  $80^\circ\text{C}$  for 2 days are obtained, as shown in Fig. 6. No trace of Au crystal diffraction peaks for  $\text{Au}^{3+}(\text{H}_2\text{O})$  can be detected after drying process (see curve-a). While the diffraction peaks, corresponding to (111), (200), (220) and (311) planes of Au crystal, can be seen for the  $\text{Au}^{3+}(\text{H}_2\text{O})\text{-PVP}$  gel (see curve-b), indicating the formation of Au nanocrystals with rich (111) plane.

As evidenced by the above experimental results, we got some opinions on the reduction of metal ions. (1) The EG molecule has no reduction effect on metal ions at room temperature, because the hydroxy groups in EG molecule have no reduction property for metal ions (that is why solutions of  $\text{AgNO}_3$  and  $\text{HAuCl}_4$  dissolved in EG can be kept stable for several months); (2) Without the application of PVP,  $\text{Ag}^+$  ions can be reduced by glycollic aldehyde that oxidated from EG molecules in a hot system (such as  $150^\circ\text{C}$ ), while the reduction of  $\text{Au}^{3+}$  ions in this system takes place very slowly. (3) At temperature  $< 100^\circ\text{C}$ , PVP polymer plays a reduction effect on metal ions.

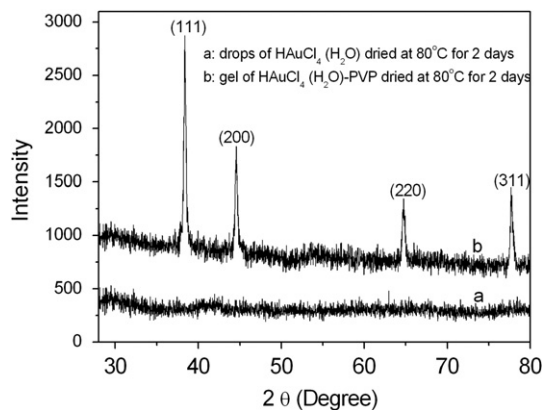
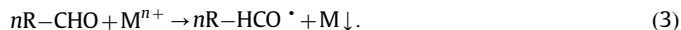


Fig. 6. XRD patterns for  $\text{Au}^{3+}(\text{H}_2\text{O})$  without (curve-a) and with (curve-b) the use of PVP dried at  $80^\circ\text{C}$  loaded on glass slides.

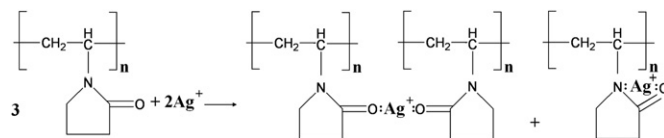
### 3.4. PVP roles as reducing agent and shape controller

As a water-soluble polymer, PVP possesses generic characteristics such as adhesiveness, absorbency, solubilization, condensation, biological compatibility and complexity. It is broadly used in areas such as medicine, food, cosmetics and health-related domains. In our recent work, we have also taken advantages of the properties of PVP and found that PVP plays an important role in determining the final shape of nanocrystals. Briefly, it is known that PVP has affinity toward many chemicals to form coordinative compounds because it has structure of a polyvinyl skeleton with strong polar pyrrolidone ring. As it is known that metal ions can be reduced by aldehyde groups through the reaction:



From the organic chemistry, it is suggest that electron clouds strongly partial to oxygen in the polar carbonyl group ( $\text{C=O}$ ), and nitrogen atom transfers its electrons to pyrrolidone ring of PVP. Correspondingly, chemical reaction can take place between PVP and metal ions, in which metal ions receive lone pair of electrons from the ligand of  $\text{-N}$  and  $\text{C=O}$  in pyrrolidone ring and form atomic metal that further grow into particles. For the gel of  $\text{Ag}^+(\text{H}_2\text{O or EG})\text{-PVP}$  kept at room temperature, the sp hybridized  $\text{Ag}^+$  ions in the coordinative complex get electrons from both oxygen and nitrogen atoms of PVP and form Ag atoms as Scheme 1 [29].

After a short incubation time, the Ag atoms form crystal nuclei and grow further into Ag nanoparticles. From the general field of colloid chemistry, it is known that fast reduction/nucleation relative to growth results in small particle with a narrow size distribution [38]. The fast reduction of  $\text{Ag}^+$  ions induces Ag atoms with high concentration. Then the Ag atoms form a large number of nuclei which provide “seeds” for further attachment of the neighbor Ag atoms. As mentioned in Ref. [29], once PVP was mixed with  $\text{AgNO}_3$  with EG as solvent, the coordination complex compound would promote a relatively fast formation of Ag nanoparticles. At the same time, the excessive PVP coverage on the surfaces of Ag nuclei would induce a simultaneous growth for different crystal faces to Ag nanoparticles with small sizes (Fig. 3(d)). Compared with the reduction of  $\text{Ag}^+$  ions in  $\text{Ag}^+(\text{EG})\text{-PVP}$ , the reduction rate of  $\text{Ag}^+$  ions in  $\text{Ag}^+(\text{H}_2\text{O})\text{-PVP}$  is relatively slow, as indicated by the color changes and optical spectra of 3# and 4# gels (Figs. 1 and 2), especially for the samples in initial stage. Then the slow reduction rate of ions in water system would lead to the growth competition between single crystal and twinned particles, as discussed in the following part about the growth of Au nanostructures. Therefore, the different reduction rates of  $\text{Ag}^+$  ions in 3# and 4# gels result in the formation of Ag nanoparticles with different sizes and shapes, which in turn bring difference on the optical absorption spectra for the final product, as inserted in Fig. 2(b) and (c). Furthermore, in the study of the growth mechanism of nanostructures fabricated by polyol process, it is generally believed that the bonding between PVP and the metal remains even when the metal ions are reduced, particular for the case of Ag (Although the exact bonding geometry and the nature of the selectivity between different crystallographic planes are still not clear). That is why the colloids



Scheme 1. Complexation of Ag ions with PVP chains.

of Ag nanostructures can be kept stable for a long time even after centrifugation with water for several times.

As for the  $\text{HAuCl}_4(\text{H}_2\text{O}$  or EG)-PVP system, the ability of PVP to reduce  $\text{Au}^{3+}$  ions into  $\text{Au}_0$  and the formation of Au nanostructures are much lower than that for  $\text{Ag}^+$  ions. Usually, it is suggested that because  $\text{HAuCl}_4$  solution has strong acidity, only a very few free  $\text{Au}^{3+}$  ions were ionized from the stable complex  $\text{AuCl}_4^-$  ions at room temperature (the probability of  $\text{Au}^{3+}$  ions ionized from  $\text{AuCl}_4^-$  ions increases with temperature). As a result, the complete reduction of  $\text{Au}^{3+}$  ions in  $\text{HAuCl}_4$  needs a long time. The experimental results that the color change (yellow to colorless) and the disappearance of 320 nm peak but no SPR of Au nanoparticles in the optical spectra suggest the reduction process of  $\text{Au}^{3+}$  ions involves two clear stepwise reduction stages of  $\text{Au}^{3+} \rightarrow \text{Au}^+ \rightarrow \text{Au}$ , which is similar to the behavior of  $\text{HAuCl}_4$  mixed with weak reducing agents, such as aniline, ascorbic acid and oleylamine [32–36]. Because slow reduction of  $\text{Au}^{3+}$  ions will induce Au atoms with low concentration, only a small number of Au nuclei formed in the gel. Since the formation of a stable Au nuclear needs a certain number of Au atoms, the as-reduced Au atoms and/or the subsequent formed Au atoms will not form new Au nuclei, but preferentially diffuse onto the nearby formed Au “seeds” due to the existence of Au atomic concentration gradient around them. In the process of chemical synthesis with the presence of PVP, the growth of Au crystals was often controlled kinetically rather than thermodynamically. The surface energy difference on crystal plane and preferential absorption of PVP on a certain plane confers the tendency to nucleate and grow into anisotropic nanoparticles, as discussed elsewhere [22]. Briefly, because PVP polymer possesses a hydrophilic polar groups, they will interact preferentially on the sites of the (111) plane of Au crystal by chemical adsorption, which obviously slows (or prevents) the growth on the (111) plane and promotes a highly anisotropic crystal growth. A platy morphology is achieved by suitable PVP capping on a pair of {111} basal faces. The side walls of the plates are inferred to be surrounded by three pairs of {110} planes because the planes are vertically arranged to the {111} faces and composed of a highly packed lattice. At the sites of thick PVP concentration, PVP would induce additional capping of the side {110} faces, which changes the growth behavior from two-dimensional expansion to one-dimensional elongation into nanobelts along a specific direction. Additionally, if the metal precursor was not mixed uniformly with PVP polymer, in some parts of the gel, the excessive PVP coverage on the surfaces of Au particles would induce a simultaneous growth for different crystal faces to some extent (or even growth limitation) apart from the anisotropic growth within the (111) plane, leading to the formation of multi-shaped Au nanostructures.

Here, we must point out that no such reduction rate could be made purely on the particle size and shape distribution. During the crystal growth in an open environment, the systems are undergoing the different processes of Ostwald ripening, particle migration and coalescence under certain conditions. As it is known that PVP polymer plays a non-negligible role on the characteristic of the final products at a certain condition, especially for Ag nanostructures (PVP is selectively capped on the {100} for Ag crystal, but {111} for Au crystal). Additionally, our experiment was carried out at different seasons, dissolving speed of PVP at different temperature, viscosity difference between EG and water, as well as the flowability difference of gels might also affect the crystal growth and in turn the final morphology of nanostructures.

In the case of the star-like Au nanoplates obtained with suitable growth disturbance, our initial analysis and theoretical calculations indicate that the lateral facets should be dominated by (110) and (211) planes. Further experiments and analysis are

now proceeding. A series of results will be delivered in a forthcoming paper.

#### 4. Conclusions

In summary, this article presents the reduction mechanisms of metal ions in the gels through study on the color changes and the corresponding optical spectra. Through comparing the results, we get some understandings on the reduction of  $\text{Au}^{3+}$  and  $\text{Ag}^+$  ions, especially in the polyol process that was widely applied to fabricate metal nanostructures. (1) EG molecule has no reduction effect at room temperature. (2) In a hot system,  $\text{Ag}^+$  (but not  $\text{Au}^{3+}$ ) ions can be easily reduced by the reducing agent decomposed from EG molecules. The role of EG was investigated by Raman spectra wherein EG plays the role of reducing agent thereby getting oxidized into carbonyl species. (3) At temperatures  $< 100^\circ\text{C}$ , PVP polymer plays an important reduction effect on metal ions. (4) The reduction effect of PVP is strong on free  $\text{Ag}^+$  ions in  $\text{AgNO}_3$ , while the reduction of complex  $\text{Au}^{3+}$  ions in  $\text{HAuCl}_4$  involves two long-time stepwise reduction stages of  $\text{Au}^{3+} \rightarrow \text{Au}^+ \rightarrow \text{Au}$ . The differences in particles size and shape are also discussed from colloid chemistry. Au nanoplates with a new and interesting star-like shape were also mass-synthesized. This work is valuable for understanding the role of PVP on the formation of metal nanostructures and the new well-defined Au nanoplates will open a new sight on the mechanics of nanostructures growth.

#### Acknowledgments

This work was financially supported from the National Natural Science Foundation of China (Grant nos. 10704038 and 10772084). We thank Dr. Zhaosheng Li and Dr. Changhui Xu of Nanjing University for their great help with the XRD and Raman spectra measurements.

#### References

- [1] U. Krebig, M. Vollmer, Theoretical considerations—single clusters: intrinsic size effects of the optical properties, in: *Optical Properties of Metal Clusters*, 1995, Springer, Berlin and Heidelberg, Germany, p. 83.
- [2] C.F. Bohren, D.R. Huffman, *Surface modes in small particles*, in: *Absorption and Scattering of Light by Small Particles*, 1983, Wiley, New York, p. 373.
- [3] J. Turkevich, P.C. Stevenson, J. Hillier, *Faraday Soc.* 11 (1951) 55.
- [4] L.M. Liz-Marzán, *Mater. Today* (2004) 26.
- [5] A.R. Tao, S. Habas, P. Yang, *Small* 4 (2008) 310.
- [6] P. Zijlstra, J.W.M. Chon, M. Gu, *Nature* 459 (2009) 410.
- [7] R.C. Jin, Y.W. Cao, C.A. Mirkin, K.L. Kelly, G.C. Schatz, J.G. Zheng, *Science* 294 (2001) 1901.
- [8] M. Maillard, S. Giorgio, M.P. Pileni, *J. Phys. Chem. B* 107 (2003) 2466.
- [9] K.L. Kelly, E. Coronado, L. Zhao, G.C. Schatz, *J. Phys. Chem. B* 107 (2003) 668.
- [10] D.A. Stuart, A.J. Haes, C.R. Yonzon, E.M. Hicks, R.P. Van Duyne, *IEE Proc. Nanobiotechnol.* 152 (2005) 13.
- [11] J. Perez-Juste, I. Pastoriza-Santos, M. Liz-Marzán, P. Mulvaney, *Coord. Chem. Rev.* 249 (2005) 1870.
- [12] S.E. Skrabalak, J. Chen, L. Au, X. Lu, X. Li, Y. Xia, *Adv. Mater.* 19 (2007) 3177.
- [13] A. Wijaya, K. Hamad-Schifferli, *J. Am. Chem. Soc.* 130 (2008) 8175.
- [14] N.P. Praetorius, T.K. Mandal, *Recent Patents on Drug Delivery & Formulation*, vol. 1, 2007, p. 37.
- [15] Y.G. Sun, Y.D. Yin, B. Mayers, T. Herricks, Y.N. Xia, *Chem. Mater.* 14 (2002) 4736.
- [16] Y. Sun, B. Gates, B. Mayers, Y. Xia, *Nano Lett.* 2 (2002) 165.
- [17] K.K. Caswell, C.M. Bender, C.J. Murphy, *Nano Lett.* 3 (2003) 667.
- [18] B. Wiley, Y. Sun, J. Chen, H. Cang, Z.Y. Li, X. Li, Y. Xia, *MRS Bull.* 30 (2005) 356.
- [19] F. Fievet, J.P. Lagier, B. Blin, *Solid State Ionics* 32/33 (1989) 198.
- [20] F. Bonet, V. Delmas, S. Grugeon, R.H. Urbina, P.Y. Silvert, K. Tekaia-Elhissien, *Nanostruct. Mater.* 11 (1999) 1277.
- [21] C.J. Murphy, T.K. Sau, A.M. Gole, C.J. Orendorff, J. Gao, L. Gou, S.E. Hunyadi, T. Li, *J. Phys. Chem. B* 109 (2005) 13857.
- [22] C.X. Kan, X.G. Zhu, G.H. Wang, *J. Phys. Chem. B* 110 (2006) 4651.
- [23] C.X. Kan, J.J. Zhu, X.G. Zhu, *J. Phys. D Appl. Phys.* 411 (2008) 55304.
- [24] Y. Xia, Y. Xiong, B. Lim, S.E. Skrabalak, *Angew. Chem. Int. Ed.* 48 (2009) 60.

- [25] J.E. Millstone, S.J. Hurst, G.S. Métraux, J.I. Cutler, C.A. Mirkin, *Small* 5 (2009) 646.
- [26] K. Patel, S. Kapoor, D.P. Dave, T.J. Mukherjee, *Proc. Indian Acad. Sci. Chem. Sci.* 117 (2005) 53.
- [27] I. Pastoriza-Santos, L.M. Liz-Marzán, *Adv. Funct. Mater.* 19 (2009) 679.
- [28] S.E. Skrabalak, B.J. Wiley, M. Kim, E.V. Formo, Y. Xia, *Nano Lett.* 8 (2008) 2077.
- [29] J. Bregado-Gutiérrez, A.J. Saldivar-García, H.F. López, *J. Appl. Polymer Sci.* 107 (2008) 45.
- [30] S. Giuffrida, L.L. Costanz, G. Ventimiglia, C. Bongiorno, *J. Nanopart. Res.* 10 (2008) 1183.
- [31] K. Esumi, J. Hara, N. Aihara, K. Usui, K. Torigoe, *J. Colloid Interface Sci.* 208 (1998) 578.
- [32] Z. Guo, Y. Zhang, A. Xu, M. Wang, L. Huang, K. Xu, N. Gu, *J. Phys. Chem. C* 112 (2008) 12638.
- [33] B.P. Khanal, E.R. Zubarev, *Angew. Chem. Int. Ed.* 46 (2007) 2195.
- [34] H.L. Wu, C.H. Chen, M.H. Huang, *Chem. Mater.* 21 (2009) 110.
- [35] O.C. Compton, F.E. Osterloh, *J. Am. Chem. Soc.* 129 (2007) 7793.
- [36] Z. Huo, C. Tsung, W. Huang, X. Zhang, P. Yang, *Nano Lett.* 8 (2008) 2041.
- [37] Z.S. Li, C.X. Kan, W.P. Cai, *Appl. Phys. Lett.* 82 (2003) 1392.
- [38] Z. Zhang, B. Zhao, L. Hu, *J. Solid State Chem.* 121 (1996) 105.